Temporal clustering analysis of cerebral blood flow activation maps measured by laser speckle contrast imaging

Qian Liu
Zheng Wang
Qingming Luo
Huazhong University of Science and Technology
Key Laboratory of Biomedical Photonics
of Ministry of Education
Wuhan 430074, China
E-mail: qluo@mail.hust.edu.cn

Abstract. Temporal and spatial orchestration of neurovascular coupling in brain neuronal activity is crucial for comprehending the mechanism of functional cerebral metabolism and pathophysiology. Laser speckle contrast imaging (LSCI) through a thinned skull over the somatosensory cortex is utilized to map the spatiotemporal characteristics of local cerebral blood flow (CBF) in anesthetized rats during sciatic nerve stimulation. The time course of signals from all spatial loci among the massive dataset is hard to analyze, especially for the thousands of images, each of which composes millions of pixels. We introduce a temporal clustering analysis (TCA) method, which is proven as an efficient method to analyze functional magnetic resonance imaging (fMRI) data in the temporal domain. The timing and location of CBF activation shows that contralateral hindlimb sensory cortical microflow is activated to increase promptly in less than 1 s after the onset of 2-s electrical stimulation and is evolved in different discrete regions. This pattern is similar but slightly elaborated from the results obtained from laser Doppler flowmetry (LDF) and fMRI. We present this combination to investigate interacting brain regions, which might lead to a better understanding of the nature of brain parcellation and effective connectivity. [DOI: 10.1117/1.1891105]

Keywords: temporal clustering analysis; cerebral blood flow; laser speckle contrast imaging; somatosensory cortex; laser Doppler flowmetry; functional magnetic resonance imaging.

Paper 04087 received Jun. 1, 2004; revised manuscript received Aug. 23, 2004; accepted for publication Sep. 1, 2004; published online Apr. 29, 2005. Portions of this paper were presented at the SPIE Conference on Complex Dynamics, Fluctuations, Chaos, and Fractals in Biomedical Photonics, Jan. 2004, San Jose, California. The paper presented there appears (unrefereed) in SPIE Proceedings Vol. 5330.

1 Introduction

Cerebral blood flow (CBF) changes resulting from brain functional activation are an important component of the hemodynamic response. Monitoring the temporal and spatial changes of CBF is crucial to comprehending the mechanism of functional cerebral metabolism and pathophysiology. At present there are several techniques for CBF velocity measurement. Laser-Doppler flowmetry (LDF) is typically used for blood flow monitoring and provides high temporal resolution measurements of relative blood flow changes from a limited number of isolated points in the brain (approximately 1 mm^3).[1,2] While scanning laser-Doppler systems can be used to obtain spatially resolved relative CBF images, their temporal resolution is insufficient for imaging the cerebral blood flow response to most functional stimuli due to the need for scanning,[3,4] such as laser-Doppler perfusion imaging (LDPI). Another method is time-varying laser speckle,[5,6] which also suffers from the limitation of measurement on a single point. Therefore, a noninvasive CBF monitoring method that does not suffer from either limited spatial resolution, temporal resolution, or a combination thereof, would be helpful in experimental investigations of functional cerebral activation.

One technique is the laser speckle imaging technique (LSI) using the first-order spatial statistics of time-integrated speckle, which was first proposed by Fercher and Briers,[7,8] and further developed by a few groups.[5,9] They demonstrated that the motion information of the scattering particles could be determined by integrating the intensity fluctuations in a speckle pattern over a finite time. The speckle method has been used to image blood flow in the retina[10] and skin.[11] Lately, the group at Harvard medical school applied this method to image blood flows during focal ischemia and cortical spreading depression (CSD).[12,13] In previous reports,[14–16] we developed a modified laser speckle imaging method that is based on the temporal statistics of a time-integrated speckle. The spatial and temporal resolutions of this method were

Address all correspondence to Qingming Luo, Biomedical Engineering, Huazhong University of Science & Technology, The Key Lab of Biomedical Photonics-College of Life Science and Technology, Wuhan, Hubei 430074 China.

1083-3668/2005/$22.00 © 2005 SPIE

studied in theory and compared with laser speckle contrast analysis (LASCA).[15]

We investigated the spatiotemporal characteristics of changes in cerebral blood volume associated with neuronal activity in the hindlimb somatosensory cortex of α-chloralose-urethane anesthetized rats with optical imaging at 570 nm through a thinned skull.[17] Activation of the cortex was carried out by electrical stimulation of the contralateral sciatic nerve with 5-Hz, 0.3-V pulses (0.5 ms) for 2 s. The stimulation evoked a monophasic decrease in optical reflectance at the cortical parenchyma and arterial sites soon after the onset of stimulation, whereas no similar response was observed at vein compartments. Another group[12] also demonstrated that LSI can monitor the cerebral blood flow (CBF) behaviors with regard to neural mechanisms of brain events under the normal and pathophysiologic conditions, which offered far better spatial and temporal resolution than most alternative imaging techniques thus far. However, it is awkward to show the time course of signals from all spatial loci among the massive dataset, especially when we had to deal with thousands of images, each of which is composed of millions of pixels. Fortunately, temporal clustering analysis (TCA) was proved to be an efficient method to analyze functional magnetic resonance imaging (fMRI) data in the temporal domain.[18]

We used TCA to analyze the data from LSI high-resolution optical imaging. TCA is based on a probability distribution of the overall brain voxels that concurrently reach extreme intensity change of imaging signals, which define a group of maximal pixels at a certain moment (N_{max}) as a temporal cluster. Mathematically, TCA avoids complicated computation, since it converts a multiple-dimension data space into a simple relationship between the number of pixels and the time. Unlike other paradigm-dependent methods, this method does not require the slightest idea of prior assumptions or knowledge regarding the possible activation patterns. As an example, we present this novel statistical analysis method to resolve the temporal evolution of evoked CBF changes across the somatosensory cortex during sciatic nerve stimulation.

2 Material and Methods

2.1 *Animal Preparations*

All animal experiments were performed within the guidelines for neuroscience research. Ten adult male Sprague-Dawley rats (350 to 400 g, Animal Research Center in Hubei, China) were initially anesthetized with 2% halothane. The right femoral vein was cannulated for drug administration and the right femoral artery for measurement of mean arterial blood pressure (PcLab Instruments, China). A tracheotomy was executed to enable mechanical ventilation with a mixture of air and oxygen (20% O_2, 80% N_2, TKR-200C, China). Periodically, blood gases/acid number were analyzed and kept at physiological arterial blood levels of PaO_2, $PaCO_2$, and pH (JBP-607, Dissolved Oxygen Analyzer, China). The animals were mounted in a stereotaxic frame, and rectal temperature was maintained at 37.0 ± 0.5 °C with a thermostatic heating blanket. Anesthesia was continued with an intraperitoneal injection of α-chloralose and urethane (50 and 600 mg/kg, respectively). The skull overlying the hindlimb sensory cortex (2.46×3.28 mm) caudal and lateral to the bregma[19] was bored to translucency with a saline-cooled dental drill, as shown in Fig. 1(a). Supplemental doses (one-fifth initial dose) were administered hourly, and atropine (0.4 ml/kg sc) was needed to reduce mucous secretions during surgery. The contralateral sciatic nerve was dissected free and cut proximal to the bifurcation into the tibial and peroneal nerves. Then the proximal end was placed on a pair of silver electrodes and bathed in a pool of warm mineral oil.

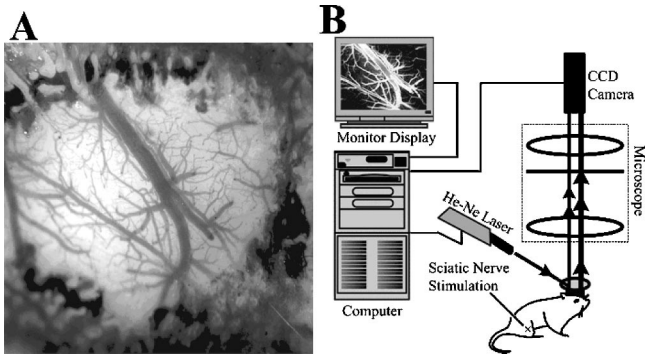

Fig. 1 (a) Location of active region. (b) Schematic of system for laser speckle contrast imaging. The light beam from a He-Ne laser was coupled with a stereo microscope through an 8-mm-diam fiber, which was adjusted to illuminate the area of interest evenly and generated images by a CCD camera.

2.2 *Laser Speckle Imaging System*

The speckle contrast imaging instrument is shown in Fig. 1(b). The light beam from a He-Ne laser ($\lambda=632.8$ nm, 3 mw, Melles Griot, CA) was coupled with a stereo microscope (SZ6045, Olympus, Japan) through an 8-mm-diam fiber bundle. The illuminated area was imaged onto a CCD camera (Pixelfly, PCO Computer Optics, Germany) with 640×480 pixels. The single sciatic nerve on the left was stimulated 2 s with rectangular pulses of 0.5-ms duration, 350-mV intensity, and 5-Hz frequency (Multi Channel Systems, Germany). For each animal, a single-trial procedure was repeated 15 to 20 times and separated by an interval of at least 4 min. 400 frames of raw images were obtained in 10-s single trials, while the electrical stimuli started at 2 s and the images in the first 2 s were recorded as baseline. Images were acquired through Easy-Control software (PCO Computer Optics, Germany) at 40 Hz and synchronized with Multi Channel Systems. Notably, data acquisition was synchronized with the electrical signal via an appropriate trigger circuit, and therefore the procedures of data analysis described later could improve the reproducibility of our results and enhance the signal-to-noise ratio.[20]

2.3 *Data Processing Methods*

2.3.1 *OTCA and MTCA*

The raw LSCI images were processed with the algorithm of LASCA described in detail by Dunn et al.[12,14,21] Relative velocities of capillary blood and cerebral blood flow maps were obtained according to the relationship between the speckle contrast and correlation time. To seek the maximal brain responses from a population of brain activation images, Liu et al.[18] and Yee and Gao[22] have presented origin TCA

(OTCA)[18] and modified TCA (MTCA)[22] algorithms for time course fMRI images. We applied the OTCA and MTCA algorithms in laser speckle contrast images to analyze the temporal and spatial CBF changes that occurred in optical images.

The LSCI sequences (images with $x \times y$ spatial pixels at time point t) were built into a multidimension data matrix $\mathbf{S}(x,y,t)$ as follows:

$$\mathbf{S}(x,y,t)=\begin{pmatrix} S_{1,1} & S_{1,2} & S_{1,3} & \cdots & S_{1,t} \\ S_{2,1} & S_{2,2} & S_{2,3} & \cdots & S_{2,t} \\ S_{3,1} & S_{3,2} & S_{3,3} & \cdots & S_{3,t} \\ \vdots & \vdots & \vdots & \cdots & \vdots \\ S_{x\times y,1} & S_{x\times y,2} & S_{x\times y,3} & \cdots & S_{x\times y,t} \end{pmatrix}. \tag{1}$$

The matrix element $\mathbf{S}_{i,j}$ is given by the pixel value at the i'th spatial and j'th temporal position $(1 \leqslant i \leqslant x \times y, 1 \leqslant j \leqslant t)$. For OTCA, the matrix $\mathbf{S}_{i,j}$ is normalized with the baseline pixel value $S_{i,0}$ and replaced with the same dimensional matrix $\mathbf{V}^O_{i,j}$:

$$\mathbf{V}^O_{i,j}=\frac{|S_{i,j}-S_{i,0}|}{S_{i,0}}(1 \leqslant i \leqslant x \times y, 1 \leqslant j \leqslant t). \tag{2}$$

While for MTCA, matrix $\mathbf{V}^M_{i,j}$ is constructed without any normalization process from the matrix $\mathbf{S}_{i,j}$:

$$\mathbf{V}^M_{i,j}=\mathbf{S}_{i,j}(1 \leqslant i \leqslant x \times y, 1 \leqslant j \leqslant t). \tag{3}$$

To track the extreme signals on the pixel-wise LSCI time series, there is a selection criterion that states whether a pixel at the i'th spatial point reached maximum at the j'th time point among the whole changes in time. From matrix $\mathbf{V}^O_{i,j}$ of OTCA, a transient matrix $\mathbf{W}^O_{i,j}$ with the same dimension can be obtained using the following selection criterion:

$$\mathbf{W}^O_{i,j}=\begin{cases} 1, & \text{if } \mathbf{V}^O_{i,j}=\max\{V^O_{i,1},V^O_{i,2},V^O_{i,3},\cdots,V^O_{i,t}\} \\ 0, & \text{otherwise} \end{cases}. \tag{4}$$

However, the selection criterion of MTCA is weighted by the intensity of the original pixel. Therefore, the transient matrix $\mathbf{W}^M_{i,j}$ of MTCA can be obtained as follows:

$$\mathbf{W}^M_{i,j}=\begin{cases} \mathbf{V}^M_{i,j}, & \text{if } V^M_{i,j}=\max\{V^M_{i,1},V^M_{i,2},V^M_{i,3},\cdots,V^M_{i,t}\} \\ 0, & \text{otherwise} \end{cases}. \tag{5}$$

$\mathbf{W}^O_{i,j}$ and $\mathbf{W}^M_{i,j}$ are the extreme pixels at the diverse time point. Furthermore, the sum of those extreme pixels at each time point t generate 1-D temporal changes in pattern K^O_j and K^M_j:

$$K^O_j=\sum_{i=1}^{x\times y} W^O_{i,j} \quad \text{and} \quad K^M_j=\sum_{i=1}^{x\times y} W^M_{i,j}. \tag{6}$$

Consequently, the plots of K^O_j and K^M_j against time points can be used to detect time windows of activation peaks without assuming the temporal response pattern of the brain. The difference between OTCA and MTCA is the recording method of maximum pixels. OTCA is based on the number of pixels of a temporal cluster, while MTCA is based on the integrated signal intensity of a temporal cluster at each time point.

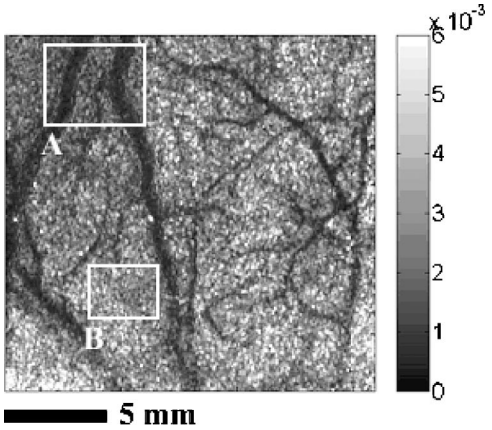

Fig. 2 Blood flow pattern from a laser speckle contrast image. ROI-A represents the area of a larger blood vessel. ROI-B represents the area of the blood vessel bed.

2.3.2 *Simulation of noisy LSCI images in time series and activation patterns*

To generate simulated LSCI image data, a single image with cerebral blood capillaries was selected (Fig. 2). Due to the fact that the maximum value is computed in TCA, LSCI image data should be converted to reciprocal on account of that the minimum value of the image (darker) represents the fast velocity. The pixels number of one image is 95×127. Two regions of interest (ROIs), ROI-A and ROI-B, were selected to represent different locations of cerebral blood vessel. The number of pixels in ROI-A and ROI-B were 720 and 370, respectively. $95\times127\times150$ (x,y,t) random data points following a Gaussian distribution (mean=0, standard deviation=1) were generated using Matlab software (version 6.0, MathWorks, Natick, MA) to create 150 noise images simulated in a time series. The maximum contrast-to-noise ratio (CNR=I/σ, where I is the activation intensity, and σ is the noise level) varied from 1 to 5 when the noise level was 1% and maximum signal change in the ROI ranged from 1 to 5%. ROI-A and ROI-B were assumed as the brain activation zones in time series images. Activation intensities were set to 1, 3, and 5%, respectively, and occurred at the time points of 30 to 45 in ROI-B and 70–85 in ROI-A, as shown in Figs. 3(a), 3(b), and 3(c).

2.3.3 *Data processing*

Both OTCA and MTCA methods were applied separately for each of the activation patterns. Normalized maximal pixel numbers ($N_{\max}$) defined as the normalized K^O_j or K^M_j in Eq. (6) is plotted against time points as shown in Figs. 3(d), 3(e), and 3(f) for OTCA; and 3(g), 3(h), and 3(i) for MTCA, where the peak of simulated brain activations can be visually detected. In the condition of low CNR (CNR=1), both OTCA and MTCA methods cannot distinguish the signal from noise. When CNR=3 or CNR=5, OTCA can distinguish the activations in ROI-B and ROI-A, however, MTCA misses the detection of ROI-B. Amplitude of activation response in ROI-A is approximately twice higher than that in ROI-B by OTCA,

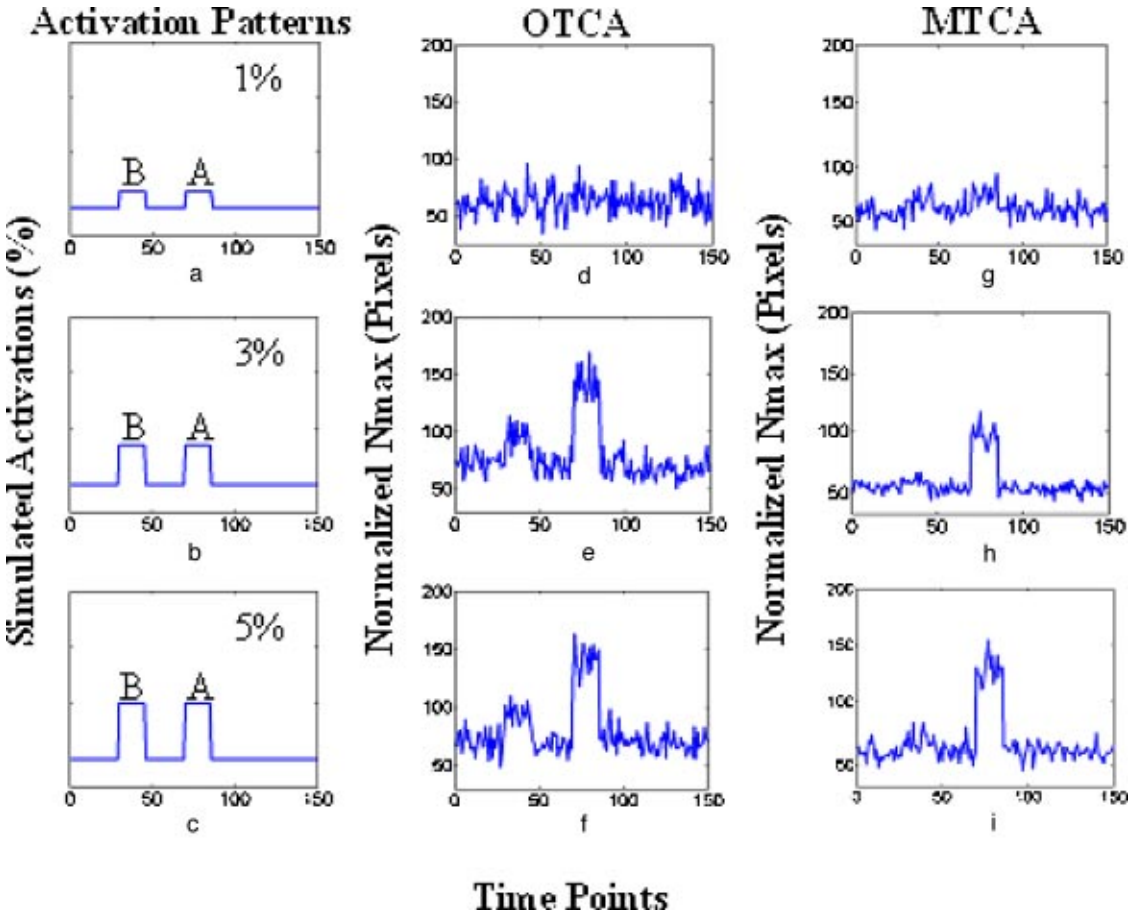

Fig. 3 Simulated activation patterns and the resulting temporal data of TCA. Activation intensity was varied from 1 to 5% by 2% increments with noise level of 1% [(a), (b), and (c)]. All plots of N_{max} were normalized to the same scale. The plots in the second columns [(d), (e), and (f)] are results of OTCA. And the third columns [(g), (h), and (i)] are the results of MTCA.

due to the fact that the statistics of the pixel number in ROI-A is approximately doubled compared with ROI-B. Inversely, the activation response area in the imaging can be determined by tracking Eqs. (6) to (1), if the activation time point is given.

3 Results

Each of the LSCI images was a data matrix of 480×640 within the field of view of a CCD camera 2.46×3.28 mm, yielding a spatial pixel size of 5.5 μm with a modified laser speckle image method. First, a speckle-contrast image [Figs. 4(c) and 4(d)] was computed for each raw speckle image [Fig. 4(b)] by the definition of speckle contrast. A template with 5×5 pixels was used. Second, a relative blood-flow image was obtained. Each set the five speckle-contrast images and multiple CBF measurements from each imaging session was averaged together for further analysis.[20] Third, since the distribution of the maximal signals was subject to random noise in a single trial, the prior averaging strategy could accommodate interindividual variations so that the temporal peaks became more reliable and distinct [Figs. 5(a) and 5(b)]. Next, the time window was determined by data fitting near these peaks with a Gaussian model function. Then a student's t-test between the pixels inside the time window and the controlled resting pixels was applied to create the spatial activation map. Finally, all the labeled locations (those extreme pixels) were superimposed on a vascular topography of the somatosensory cortex [Fig. 4(a)] by means of the Matlab software [Figs. 6(a) and 6(b)].

Compared with Fig. 4(c), the areas of low speckle-contrast values (darker areas) that indicate increased blood flow were evident in Fig. 4(d). Thus, electrical stimulation of the sciatic nerve elicited robust increases in CBF across the somatosensory cortex, which was coherent with the former conclusions obtained by LDF[23,24] and fMRI.[25] Since a large temporal and spatial heterogeneity exists in the cerebrocortical vasculature,[26] TCA was applied to seek when and where the brain will respond after extern stimuli, regardless of individual anatomic features.[18] The temporal response profile in Fig. 5(b) exhibited only a slight difference in a double peak other than a pronounced peak revealed by other techniques.[23,24] This double peak actually represented distinct localizations of CBF activation at different moments, which also demonstrated the spatial flow heterogeneity.[12,26] As illustrated in Fig. 6(a), CBF activation at the early phase is spatially localized to the capillary bed. More discrete dotted regions activated by propagation of increased neuronal activity showed CBF draining in larger vessels [Fig. 6(b)]. The results analyzed by the TCA method indicated that the whole pattern of CBF response to extern stimuli has distinct time phases and

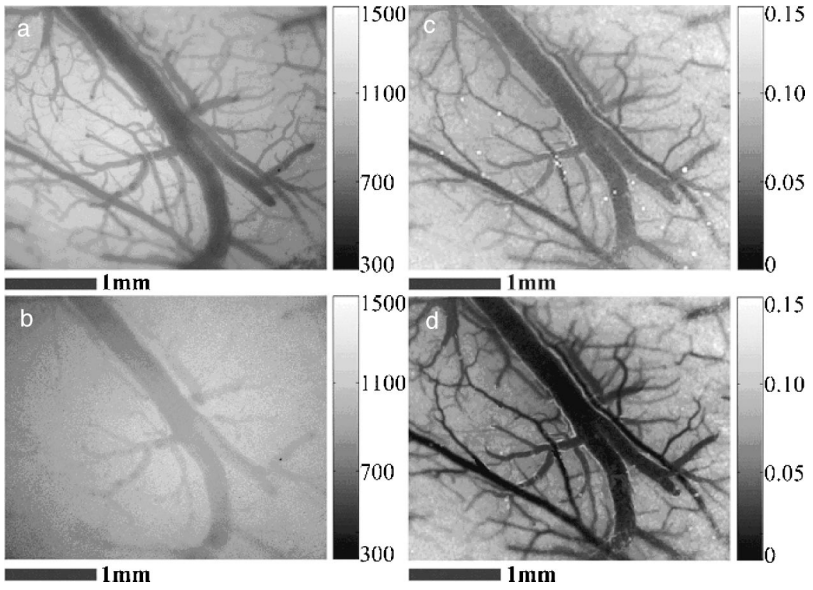

Fig. 4 LSCI of a representative animal. (a) and (b) A vascular topography illuminated with green light (540±20 nm) and a raw speckle image with laser. (a) The vascular pattern was referenced in case loss of computation occurred. (c) and (d) Speckle-contrast images under the prestimulus and poststimulus level demonstrated response pattern of cerebrocortical microflow, in which arteriolar and venous blood flow increased clearly due to sciatic nerve stimulation. The gray intensity bar (c) and (d) indicates the speckle-contrast values. The darker values correspond to the higher blood flow.

space loci, in which there are different regulation pathways to control CBF changes at different levels of blood vessels.

4 Discussion

Using the TCA method in LSCI images, we can extract the CBF activation time window and activation location in anesthetized rats during sciatic nerve stimulation. The simulation result (Fig. 3) of the activation pattern and experimental result in time-series noisy LSCI images is consistent with that in fMRI, which shows a similar time window response with simulated activation.[22] However, in LSCI, particularly in maps of blood vessels, there are minor different results due to the different intensity distribution between the OTCA and MTCA method. The OTCA method is based on the number of pixels with maximum intensity of a temporal cluster at each time point, while the MTCA method is the integrated maximum signal intensity of a temporal cluster. The OTCA method is more spatially sensitive than the MTCA method,

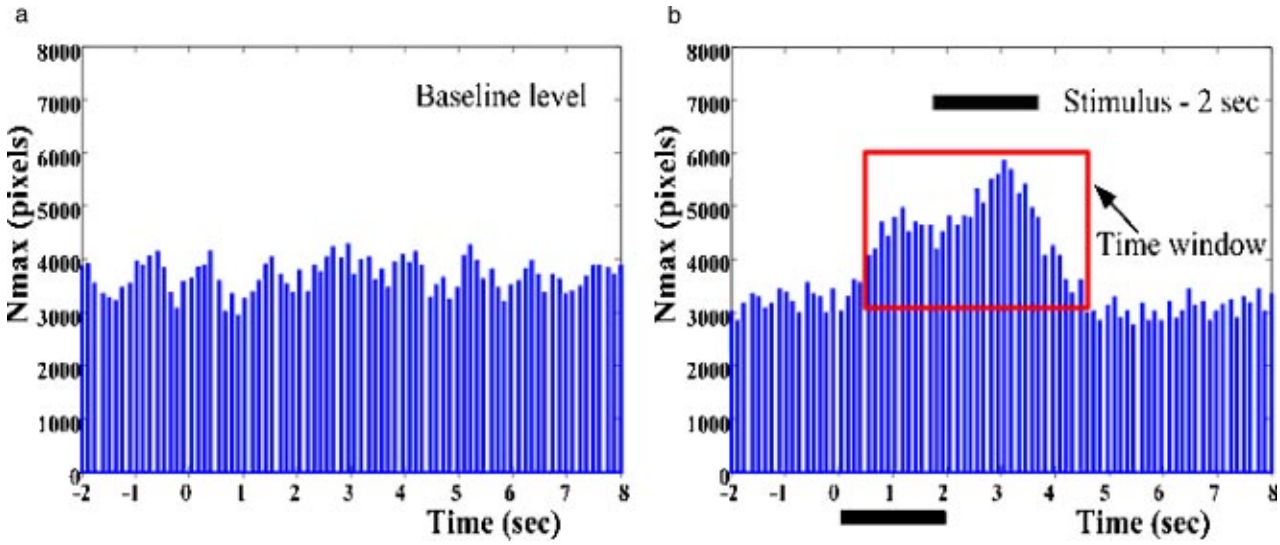

Fig. 5 N_{max} as a function of time, which stood for those pixels that reached a maximal signal at a certain moment and its value on each pixel meant the time when maximal response occurred. (a) N_{max} in control experiments without sciatic nerve stimulation, which stood for a baseline level of CBF activities embedded in all physiological and systemic noises ($n=6$). (b) Temporal maxima of CBF response to sciatic nerve stimulation. A time window (0.50±0.15 to 4.50±0.10 s) contained a double peak, 1.10±0.10 s for the first peak and 3.05±0.10 s for the second ($n=10$). The bold black line represented a stimulus of 2-s duration.

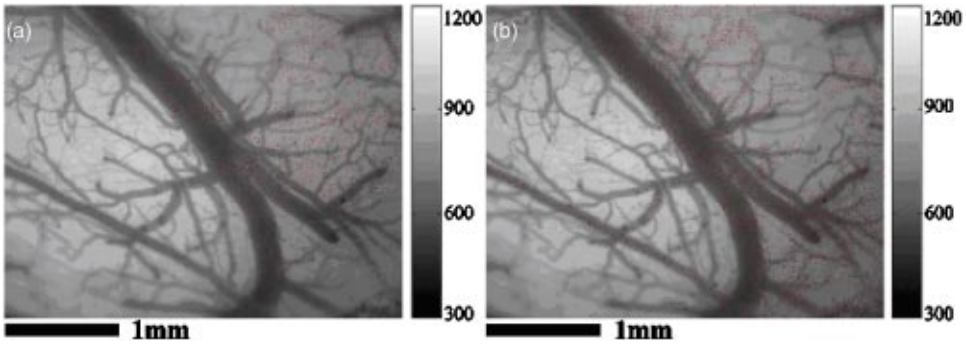

Fig. 6 Spatial activation map of CBF induced by sciatic nerve stimulation. Two representative images were selected from the relative blood flow images with labeled extreme pixels at the double peak in Fig. 5(b) to display spatial evolution of CBF response across the imaged area. (a) and (b) Activated locations of CBF at the first and second peak. The dotted areas stood for changes of CBF that reached extrema at the peak moment.

since each of the pixels, whether in a high signal intensity area or in low signal intensity area, is equal in the OTCA method, and these kinds of pixels are classified into one cluster. However, in the MTCA method, only the pixels in the high intensity area where maximum intensity occurs in a time series are classified into one cluster. As a result, the MTCA method can be applied to LSCI images, whose blood perfusion predominantly occurs in larger blood vessel (ROI-A in Fig. 2). What is more, OTCA can be applied not only in larger blood vessels but also in vessel beds that have abundant capillaries embedded under the surface membrane (ROI-B in Fig. 2). It should be pointed out that the TCA method is not suitable in the case of low CNR in laser speckle imaging and the method also reveals the same feature in fMRI.[22] Then, principal components analysis (PCA)[27] and independent components analysis (ICA)[28] should be developed to deal with this kind of laser speckle image.

In addition, a spatial activation map of CBF induced by sciatic nerve simulation can be provided by the TCA method in LSCI images according to the given time point. Although the CBF activation map in fMRI is also shown in the somatosensory cortex with a resolution of 470 μm,[25] a combination of LSCI and TCA has the ability to provide higher resolution imaging to resolve blood capillaries in the activation area. The temporal and spatial orchestration of neurovascular coupling in the brain neuronal activity is crucial for comprehending the mechanism of functional cerebral metabolism and pathophysiology. Based on high-resolution optical imaging and TCA techniques, we can extricate ourselves out of traditional paradigm-dependent studies to probe more elaborate spatiotemporal details. The second peak of the double peak acts in accord with the well-documented results that there possibly exists a rapid release of metabolic factors during the observed latency.[23,29] Thus, the behavior of regional microcirculation is genuinely adjusted to metabolic activity by chemical regulation of cerebrovascular tone mediated by the products of energy metabolism in the brain. However, the mechanism of regulating the first peak in the time window is unclear. It is almost certain that the dynamic regulation of the cerebral microcirculation is mediated by numerous neurogenic and chemical factors acting in concert.[30] Based on the fact that vascular responses to activation are extremely fast,[31] neurogenic regulation appears to represent a major role in dynamic control of the first peak. To the author's knowledge, there exist many neural vasomotor pathways in the cerebral vasculature to cause specificities in regulation of blood flow. In view of its spatial distribution localized in capillaries and microarterioles, it is presumably associated with the neurogenic regulation of coupling by classical neurotransmitters such as acetylcholine.[32] Further experiments to investigate the neurogenic effects on the cerebral vessels are needed to provide more convincing evidences.

5 Conclusions

A temporal clustering analysis technique is introduced to analyze the cerebral blood flow activation maps measured by LSCI. OTCA and MTCA methods are demonstrated using computer simulations and *in vivo* LSCI experiments. Our results suggest that the TCA method can be used to analyze brain response of laser speckle timing image.

Acknowledgments

This work was supported by grants from the National Science Foundation of China for distinguished young scholars (number 60025514), the National Science Foundation of China (number 30170306), and the Preliminary Project of the National Basic Research Priorities Program (number 2001CCA04100). The authors appreciate A. C. Ngai, P. Bandettini, L. Sokoloff, and L. Wang for their invaluable help during the preparation of this manuscript.

References

1. K. U. Frerichs and G. Z. Feuerstein, ''Laser Doppler flowmetry: a review of its application for measuring cerebral and spinal cord blood flow,'' *Mol. Chem. Neuropathol.* **12**, 55–61 (1990).
2. U. Dirnagl, B. Kaplan, M. Jacewicz, and W. Pulsinelli, ''Continuous measurement of cerebral cortical blood flow by laser-Doppler flowmetry in a rat stroke model,'' *J. Cereb. Blood Flow Metab.* **9**, 589–596 (1989).
3. B. M. Ances, J. H. Greenberg, and J. A. Detre, ''Laser Doppler imaging of activation-flow coupling in the rat somatosensory cortex,'' *Neuroimage* **10**, 716–723 (1999).
4. M. Lauritzen and M. Fabricius, ''Real time laser-Doppler perfusion imaging of cortical spreading depression in rat neocortex,'' *NeuroReport* **6**, 1271–1273 (1995).
5. D. A. Zimnyakov, J. D. Briers, and V. V. Tuchin, ''Speckle technologies for monitoring and imaging of tissues and tissuelike phantoms,'' in *Handbook of Optical Biomedical Diagnostics PM107*, V. V. Tuchin, Ed., pp. 987–1036, SPIE Press, Bellingham, WA (2002).
6. S. K. Ozdemir, S. Takamiya, S. Ito, S. Shinohara, and H. Yoshida,

''Self-mixing laser speckle velocimeter for blood flow measurement,'' *IEEE Trans. Instrum. Meas.* **49**, 1029–1035 (2000).
7. A. F. Fercher and J. D. Briers, ''Flow visualization by means of single-exposure speckle photography,'' *Opt. Commun.* **37**, 326–329 (1981).
8. J. D. Briers and S. Webster, ''Laser speckle contrast analysis (LASCA): A nonscanning, full-field technique for monitoring capillary blood flow,'' *J. Biomed. Opt.* **1**, 174–179 (1996).
9. E. I. Galanzha, G. E. Brill, Y. Aizu, S. S. Ulyanov, and V. V. Tuchin, ''Speckle and Doppler methods of blood and lymph flow monitoring,'' in *Handbook of Optical Biomedical Diagnostics PM107*, V. V. Tuchin, Ed., pp. 881–937, SPIE Press, Bellingham, WA (2002).
10. K. Yaoeda, M. Shirakashi, S. Funaki, H. Funaki, T. Nakatsue, and H. Abe, ''Measurement of microcirculation in the optic nerve head by laser speckle flowgraphy and scanning laser Doppler flowmetry,'' *Am. J. Ophthalmol.* **129**, 734–739 (2000).
11. B. Ruth, ''Measuring the steady-state value and the dynamics of the skin blood flow using the non-contact laser speckle method,'' *Med. Eng. Phys.* **16**, 105–111 (1994).
12. A. K. Dunn, H. Bolay, M. A. Moskowitz, and D. A. Boas, ''Dynamic imaging of cerebral blood flow using laser speckle,'' *J. Cereb. Blood Flow Metab.* **21**, 195–201 (2001).
13. H. Bolay, U. Reuter, A. K. Dunn, Z. Huang, D. A. Boas, and A. M. Moskowitz, ''Intrinsic brain activity triggers trigeminal meningeal afferernts in a migraine model,'' *Nat. Med.* **8**, 136–142 (2002).
14. H. Y. Cheng, Q. M. Luo, S. Q. Zeng, J. Cen, and W. X. Liang, ''Optical dynamic imaging of the regional blood flow in the rat mesentery under the drug's effect,'' *Prog. Nat. Sci.* **3**, 78–81 (2003).
15. H. Y. Cheng, Q. M. Luo, S. Q. Zeng, S. B. Chen, J. Cen, and H. Gong, ''A modified laser speckle imaging method with improved spatial resolution,'' *J. Biomed. Opt.* **8**(3), 559–564 (2003).
16. H. Y. Cheng, Q. M. Luo, Z. Wang, H. Gong, S. B. Chen, W. X. Liang, and S. Q. Zeng, ''Efficient characterization of regional mesenteric blood flow using laser speckle imaging,'' *Appl. Opt.* **42**(28), 5759–5764 (2003).
17. P. C. Li, Q. M. Luo, W. H. Luo, S. B. Chen, H. Y. Cheng, and S. Q. Zeng, ''Spatiotemporal characteristics of cerebral blood volume changes in rat somatosensory cortex evoked by sciatic nerve stimulation and obtained by optical imaging,'' *J. Biomed. Opt.* **8**(4), 629–635 (2003).
18. Y. J. Liu, J. H. Gao, H. L. Liu, and P. T. Fox, ''The temporal response of the brain after eating revealed by functional MRI,'' *Nature (London)* **405**, 1058–1062 (2000).
19. A. Alavi, R. Dann, J. Chawluk, J. Alavi, M. Kushner, and M. Reivich, ''Positron emission tomography imaging of regional cerebral glucose metabolism,'' *Semin Nucl. Med.* **16**, 2–34 (1986).
20. B. M. Ances, J. A. Detre, K. Takahashi, and J. H. Greenberg, ''Transcranial laser Doppler mapping of activation flow coupling in the rat somatosensory cortex,'' *Neurosci. Lett.* **257**, 25–28 (1998).
21. J. D. Briers, ''Laser Doppler, speckle and related techniques for blood perfusion mapping and imaging,'' *Physiol. Meas* **22**, 35–66 (2001).
22. S. H. Yee and J. H. Gao, ''Improved detection of time windows of brain responses in fMRI using modified temporal clustering analysis,'' *Magn. Reson. Imaging* **20**, 17–26 (2002).
23. T. Matsuura and I. Kanno, ''Quantitative and temporal relationship between local cerebral blood flow and neuronal activation induced by somatosensory stimulation in rats,'' *Neurosci. Res. (NY)* **40**, 281–290 (2001).
24. A. C. Ngai, J. R. Meno, and H. R. Winn, ''Simultaneous measurements of pial arteriolar diameter and laser-Doppler flow during somatosensory stimulation,'' *J. Cereb. Blood Flow Metab.* **15**, 124–127 (1995).
25. A. C. Silva, S. P. Lee, G. Yang, C. Iadecola, and S. G. Kim, ''Early temporal characteristics of cerebral blood flow and deoxyhemoglobin changes during somatosensory stimulation,'' *J. Cereb. Blood Flow Metab.* **20**, 201–206 (2000).
26. R. Steinmeier, I. Bondar, C. Bauhuf, and R. Fahlbusch, ''Laser Doppler flowmetry mapping of cerebrocortical microflow: characteristics and limitations,'' *Neuroimage* **15**, 107–119 (2002).
27. S. H. Lai and M. Fang, ''A novel local PCA-based method for detecting activation signals in fMRI,'' *Magn. Reson. Imaging* **17**, 827–836 (1999).
28. M. Mckeown, ''Detection of consistently task-related activations in fMRI data with hybrid independent component analysis,'' *Neuroimage* **11**, 24–35 (2000).
29. A. C. Ngai, K. R. Ko, S. Morii, and H. R. Winn, ''Effects of sciatic nerve stimulation on pial arterioles in rats,'' *Am. J. Physiol.* **269**, 133–139 (1988).
30. R. Greger and U. Windhorst, *Comprehensive Human Physiology*, in Vol. 1, pp. 561–578, Springer-Verlag, Berlin (1996).
31. U. Lindauer, A. Villringer, and U. Dirnagl, ''Characterization of CBF response to somatosensory stimulation: model and influence of anesthetics,'' *Am. J. Physiol.* **264**, 1223–1228 (1993).
32. M. Zimmermann, ''Ethical principles for the maintenance and use of animals in neuroscience research,'' *Neurosci. Lett.* **73**, 1 (1987).